Ascent Guidance Comparisons[1]

John M. Hanson, M. Wade Shrader, and Craig A. Cruzen[2]

Abstract

This paper contains results from ascent guidance studies conducted at the NASA Marshall Space Flight Center. The studies include investigation of different guidance schemes for a variety of potential launch vehicles. Criteria of a successful ascent guidance scheme are low operations cost, satisfaction of load indicator constraints, and maximization of performance. Results show that open-loop designs as a function of altitude or velocity are preferable to designs that are functions of time. Optimized open-loop trajectories can increase performance while maintaining load indicators within limits. Closed-loop atmospheric schemes that involve linear tangent steering or feedback of velocity terms for trajectory modification did not yield any improvement. Early release of vacuum closed-loop guidance, including use during solid rocket booster operation, yields some improvements. Evaluation of a closed-loop optimization scheme for flying through the atmosphere shows no advantages over open-loop optimization. Dispersion study results for several potential guidance schemes and launch vehicles are included in the paper and are not a discriminator between guidance schemes. The primary cost driver is mission operations philosophy, not choice of guidance scheme. More autonomous guidance schemes can help in movement towards a philosophy that would reduce operations costs.

Introduction

A good ascent guidance scheme can help by reducing cost, reducing load indicators, and increasing performance. According to a 1988 study on the Space Shuttle, about 20% of each mission's cost is due to mission design. This is not primarily due to design of trajectories, but rather to the extensive effort expended to ensure that the trajectories will be successfully flown and satisfy vehicle constraints [1]. Much of the reduction in cost that should be possible is from a change in philosophy towards mission design, rather than use of a different guidance scheme. For example, if vehicle performance envelopes are defined, ground programs can automatically verify that a given trajectory will be successful. This approach would reduce the cost by removing the need to spend

significant resources for each flight in order to be convinced of an acceptable ascent mission plan.

Traditional ascent guidance strategies employ two phases: open-loop guidance and closed-loop guidance. The open-loop segment is simply a table of attitude commands, obtained via parameter optimization, as a function of time, altitude, or velocity. These commands are optimized to give the maximum mass to orbit (performance) for a given set of constraints (mainly load constraints on the vehicle) and atmospheric conditions (density profile and winds). The closed-loop segment is usually released some time after maximum dynamic pressure. This guidance is an algorithm that resides on the flight computer and generates the attitude profile the vehicle is to follow to maximize performance to the target orbit. It does this while responding to inflight external variables, such as wind, thrust, and navigation dispersions.

Improved ascent guidance could potentially help control load indicators, by adapting to actual inflight conditions. An alternate procedure is to use day-of-launch wind design for load reduction. A combination of day-of-launch winds and an adaptive guidance might yield maximum launch availability by giving the best possible control over load indicator dispersions and might also remove the need for load-relief control. Load-relief control was shown to reduce launch availability on the Shuttle when day-of-launch wind biasing was used [1].

Improved guidance or trajectory design can also lead to increased performance (payload in orbit) through atmospheric open-loop or closed-loop optimization. During closed-loop operation, performance can be improved by adapting to actual inflight dispersions, rather than relying only on those estimated in preflight analysis.

Ground efforts associated with aborts and engine-out situations (such as the return-to-launch-site aborts of the Shuttle), and verification of trajectories, could be significantly reduced through preflight automated design or by closed-loop design onboard the vehicle.

Hanson et al. [2] investigated a number of guidance schemes and described others to be investigated. This current paper continues that investigation for a generic set of launch vehicles. Various open and closed-loop ascent guidance schemes will be compared.

Open Versus Closed-Loop Atmospheric Ascent

Presently, ascent trajectory design and validation/verification is a time and labor intensive effort. Typically, an optimized trajectory is designed using a three degree-of-freedom (3-DOF) trajectory simulator. Open-loop steering commands are determined by parameter optimization for the early portion of the flight, and a closed-loop guidance scheme determines the steering commands from closed-loop guidance release to cutoff. A 6-DOF trajectory simulation then uses the open-loop profile generated by the 3-DOF simulation to predict the loads the vehicle may encounter during flight. On most of today's launch vehicle programs, both the 3-DOF and 6-DOF simulations are verified by at least one set of independent computer programs. Also, day-of-launch (DOL) updates are used to modify the trajectory, typically by updating the predictions on the winds. Much of the cost associated with the pre-mission analysis is due to verification of these trajectories and steering commands.

Possible gains from closed-loop atmospheric ascent guidance include reduction in pre-mission analysis, reduction in load indicators, and increase in vehicle performance (mass to orbit). Since trajectory design based on DOL updates can be done regardless of whether the atmospheric guidance is open or closed-loop, closed-loop guidance will not significantly reduce load indicators. Loads resulting from vehicle dispersions are generally not large. Thus, closed-loop guidance throughout the duration of the ascent flight should not significantly improve launch availability versus open-loop guidance in the atmosphere followed by exoatmospheric closed-loop guidance.

Closed-loop guidance could adapt, by nature, to vehicle dispersions in order to achieve a trajectory that more closely follows the optimum. In the case of the Space Shuttle, the most important of these dispersions is the solid rocket booster thrust, and that dispersion is adapted to by the existing open-loop guidance scheme. It remains to be seen whether closed-loop atmospheric guidance will yield any significant performance improvement over such an open-loop technique.

One of the more labor intensive aspects of pre-mission trajectory design is contingency/abort planning. Typically, contingency trajectories must be designed during pre-mission analysis to account for abort/engine-out situations. For example, each Shuttle flight requires development of return-to-launch-site (RTLS) trajectories for differing conditions. These numerous trajectories require many labor hours of analysis for both the design and the verification of the open-loop steering profiles. A closed-loop system, which could automatically design acceptable trajectories onboard the vehicle, could save much effort by automatically adapting to the contingency situations. Some closed-loop atmospheric guidance schemes that could be used in such a manner will be considered later.

The verification process in trajectory design could be an area which can be streamlined. Presently, verification of an open-loop trajectory occurs individually; that is, each trajectory that is designed can be tested in an independent simulation to verify that it meets the criteria established for a successful trajectory. Closed-loop guidance schemes are algorithms that are part of the onboard flight software and therefore, go through a different validation process, similar to any other software that resides on the flight computer. Extensive testing occurs preflight to determine that the closed-loop guidance algorithm always produces an acceptable trajectory given the range of input data that may be used to initialize the guidance scheme, including dispersions.

If the entire trajectory design system, both the open-loop trajectory optimization program and the closed-loop scheme, could be set up so that the system can automatically determine by itself that the ascent trajectory will be successful, a significant savings in pre-mission time and effort could be achieved. It should be possible to completely automate the process of designing and verifying open-loop trajectories on the ground. An onboard method would yield fewer parameters to upload to the vehicle, however.

Ascent Guidance Options

Consider the following possible ascent guidance methods:

1. Optimized open-loop pitch and yaw profiles for atmospheric ascent, as functions of time, speed, or altitude. These are simple profiles that, for example, nominally fly zero angle-of-attack through the high dynamic pressure region.

2. Optimized open-loop profiles that allow for some nonzero angles-of-attack. The allowable load indicator values in the trajectory design may vary through the open-loop portion.

3. Closed-loop vacuum guidance. Examples are the Iterative Guidance Mode (IGM) [3] used for the Saturn vehicles, Powered Explicit Guidance (PEG) [4] used on the Shuttle, and OPGUID [5], a calculus of variations-based guidance, that has the flexibility of being useful for on-orbit operations, as well as ascent. All of these have nearly identical performance results for the vacuum portion. Typically, these guidance schemes are released just after the vehicle leaves the bulk of the atmosphere. The following schemes are variations on this method, with differing release times:

> 3a. Closed-loop vacuum guidance, released while still in the atmosphere, but after maximum dynamic pressure. Constraints can be placed on the commands, so that an attitude command that leads to an unacceptable load indicator can be modified to be acceptable. The equations ignore the atmosphere, but the constraints assure acceptable commands. Release is also possible during solid rocket burns.

> 3b. A closed-loop vacuum guidance scheme, modified to take the atmosphere into account. An example is linear tangent steering with atmospheric terms in the equations of motion [6]. This method would allow earlier release of closed-loop guidance.

4. A scheme that takes navigated dispersions (dispersions caused by winds, thrust, et cetera, that show up in the navigated state) into account during the atmospheric portion of the trajectory in an attempt to fly a more optimal trajectory. The scheme modifies the commands to try to come closer to the ground-designed optimal trajectory that would have been flown if the dispersions were known beforehand [7, 8]. This differs from method 3b, which is designing the trajectory during ascent. Method 4 is trying to fly the best trajectory that would have been designed on the ground if the dispersions were known beforehand.

5. A closed-loop scheme from lift-off that designs the trajectory as the vehicle travels, taking into account dispersions that have affected the navigated state so far. The onboard computer could converge to a solution before launch and update the solution with the latest data as the vehicle ascended. This is not an adapted vacuum scheme, but rather a completely new scheme.

Methods fitting the above descriptions will be investigated in this paper. There are varying ways to implement the above methods, and only selected versions will be examined here. For example, FAST [9] and a hybrid method using collocation and regular perturbations [10] are examples of schemes that will not be investigated, but could be applied to several of the above methods, including method 5. Other possibilities exist that will not be investigated, such as the use of neural networks for ascent guidance.

Candidate Vehicles

For the purposes of guidance comparison, four candidate launch vehicles having differing attributes were examined. These vehicles were among those considered during the National Launch System effort and the few months subsequent to that effort. The vehicles are called Early Heavy Lift Launch Vehicle (EHLLV), NLS2 with all engines running (NLS2AER), NLS2 with sustainer engine out at liftoff

(NLS2EO), and NLS3 with upper stage (NLS3US). NLS2EO is considered a separate vehicle here due to the very different ascent trajectories that result from optimizing the open-loop profiles for the vehicle with the same mission goals, but a different thrust trace. It operates with five engines at liftoff and one after staging, instead of six and two, respectively, for the NLS2AER. Besides the lower thrust-to-weight ratio, the vehicle rotates so that the bad engine is up in the pitch plane, which modifies the trajectory.

Attributes for the four vehicles are summarized in Table 1. Note that the vehicle configurations cover a range of sizes and acceleration levels. Strap-on solid boosters are included, as well as upper stages. General results should be applicable to all rocket-powered launch vehicles, including the Shuttle and proposed single-stage-to-orbit vehicles. Nominal trajectories for these vehicles are shown in Fig. 1.

Method 1: Open-Loop Guidance Comparisons

Open-loop trajectories can be designed to give tables of pitch and yaw commands, as a function of time, altitude, or velocity. The Shuttle uses Mach number, which is closely tied to velocity, as the independent variable. Analysis results shown in Table 2 demonstrate that use of time is the most sensitive

TABLE 1. Candidate Launch Vehicles[1]

Parameter	EHLLV	NLS2AER/NLS2EO	NLS3US
Vehicle mass at liftoff (kg)	2 102 641	921 076	217 782
Thrust/weight at liftoff	1.516 @ T + 1 s	1.628/1.356	1.147
Solid engines[2]	2 RSRMs	0	0
Liquid engines[2,3]	3 SSMEs	6 STMEs	1 STME (1st stage)
			1 HEUS (2nd stage)
Vehicle diameter for aerodynamics (m)	8.382	8.382	6.828
Target orbit	37 × 343 km at 51.6 deg, cutoff at 124 km	148 × 278 km at 28.5 deg, cutoff at 148 km	240 km circular at 28.5 deg
Staging time (s)	121.2 s (RSRM drop)	optimized, drop 4 engines; 127/172 s	about 218 s, run out of first-stage fuel
Drop mass at staging (kg)	171 988 (varies slightly)	35 522	21 859
Drop mass at MECO (kg) for mass in results tables	69 963	66 171	0
Shroud mass (kg)	13 542	5670	2067
Throttle for max Q	none	step to 70% from 38–80 s/none	none
Throttle for g-limit	3.2 g's continuous throttle	4.5 g's step to 70%	none

[1] Shroud drop at 121 920 m (400 000 ft). Environment (nominal): Patrick 1963 atmosphere, mean annual enveloping wind.
[2] Acronyms: RSRM–Redesigned Solid Rocket Motor (used on Shuttle; see Fig. 5 for thrust and flow rate); SSME–Space Shuttle Main Engine; STME–Space Transportation Main Engine; HEUS–High-Energy Upper Stage.
[3] Liquid engine attributes: STME–Thrust 2 891 344 N, I_{sp} 428.5 s, step throttle to 70%; SSME–Thrust 2 174 291 N, I_{sp} 452.5 s, continuous throttle; HEUS–Thrust 133 447 N, I_{sp} 455 s.
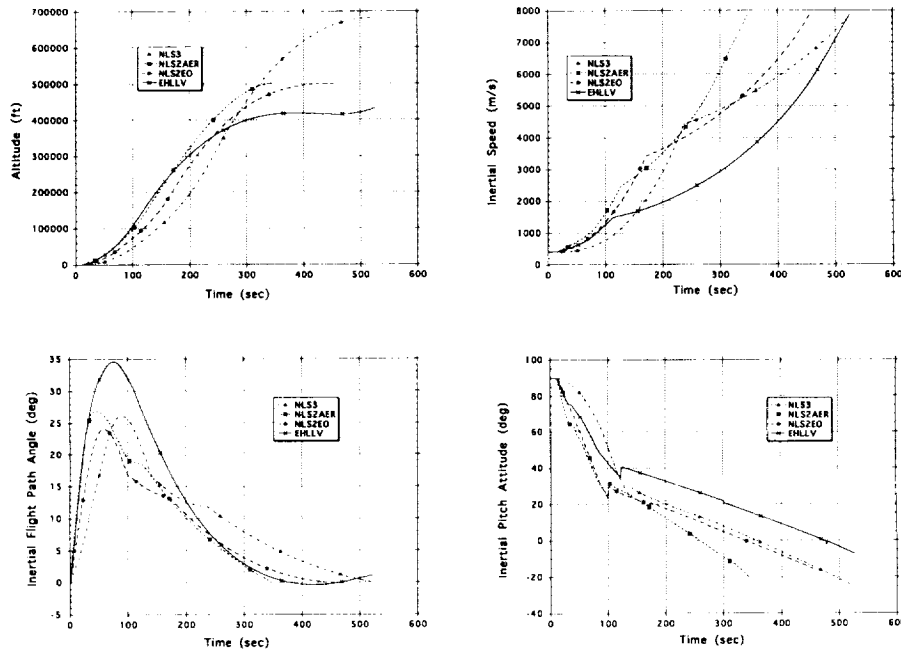
FIG. 1.   Nominal Trajectories for Four Candidate Vehicles.

parameter (varies the most with changes). Other studies agree with this result. Altitude and velocity should be less sensitive since a more sluggish vehicle will reach target altitudes and velocities later, whereas time is linear regardless of the vehicle motion.

To further examine altitude and velocity-based profiles, consider the four candidate vehicles. Two tests were used. First, each vehicle trajectory was biased to a mean annual enveloping wind and then flown to four 99% enveloping wind profiles corresponding to a maximum headwind, tailwind, and right and left crosswinds (furnished by New Technologies, Inc. under contract to MSFC). The extreme wind profiles are for a due east launch from Kennedy Space Center. Table 3 lists the mass to orbit (MECO mass) of the four vehicles biased to the four wind profiles, plus the case biased to mean annual winds, for each method of trajectory shaping: altitude-based and velocity-based. The four extreme profiles do not correspond to headwind, tailwind, et cetera, for the EHLLV, due to its high inclination orbit of 51.6 degrees.

TABLE 2.   Sensitivity Analysis of Open-Loop Guidance Methods (NLS2 with engine out)

Guidance Method	Δ Excess Propellant at MECO (lb_m)[1]	Δ Pitch Rate[1]
Pitch rate versus time	−2251	0.31
Pitch rate versus altitude	−1719	0.17
Pitch rate versus velocity	−1890	0.23

[1]Change between bias to mean annual and bias to 99% maximum headwind.

TABLE 3. Results for 99% Wind Profiles (MECO mass in pounds)

Wind Profile	EHLLV (altitude-based)	EHLLV (velocity-based)	NLS2AER (altitude-based)	NLS2AER (velocity-based)
Mean	324 890	324 870	219 100	219 130
Headwind	322 969	323 031	217 991	218 022
Tailwind	326 628	326 441	220 106	220 118
Southerly	326 407	326 291	219 340	219 318
Northerly	323 267	323 318	218 730	218 789

Wind Profile	NLS2EO (altitude-based)	NLS2EO (velocity-based)	NLS3US (altitude-based)	NLS3US (velocity-based)
Mean	209 210	209 210	33 024	33 014
Headwind	208 058	208 058	32 684	32 682
Tailwind	210 263	210 291	33 344	33 335
Southerly	209 404	209 447	33 101	33 096
Northerly	208 905	208 903	32 926	32 921

Comparing the mass to orbit numbers for the altitude-based and velocity-based cases for each vehicle shows nearly identical results between the two different methods, with velocity being slightly better. For example in the EHLLV case, the velocity-based design for headwinds was 323 031 lb_m to orbit, while the altitude-based design was 322 969 lb_m, for a difference of only 62 lb_m. This pattern of small differences between the altitude-based trajectory design and the velocity-based trajectory design can be found for all three vehicles, biased to all five wind cases. The small difference that exists could be due to slight variations in the sideslip hold points (sideslip held to zero during the high dynamic pressure region, in the design of the wind-biased trajectory) or some other similar factor.

The second test concerned day-of-launch wind biasing. For the NLS2 with all engines running, the study found results for 114 measured February day-of-launch wind pairs (furnished by New Technologies, Inc. under contract to MSFC). The first profile of each pair was measured about 3 hours before the second of the pair. The flight profile is biased to the first wind profile of each pair and then flown to the second of the pair. The criteria used to judge the cases was again the mass to orbit. Comparing the cases resulting in lowest masses to orbit, there is again very little difference between profiles designed by altitude and those designed by velocity. For the 10 wind profile cases that gave the worst performance, the differences in mass to orbit between the profile based on velocity and the profile based on altitude are 52, 21, 14, 35, −2, −4, 51, 7, 37, and 23 lb_m. Although the cases are close, the velocity results again appear to be slightly better.

Method 2: Optimized Open-Loop Trajectories with Nonzero Angle-of-Attack

Judicious design of the open-loop portion of the trajectory can maintain load indicators within limits while simultaneously improving performance. The primary load indicators of interest are the Q-α and Q-β parameters (product of dynamic pressure and aerodynamic angles). The key in designing the trajectory optimally is

not to exceed (in actual flight) the maximum values of these indicators that would be seen from wind dispersions only. If this is done, the vehicle will not require structural strengthening to satisfy the new trajectory design. Figure 2 shows a typical curve for Q-α and Q-β (resulting from wind dispersions only). At each altitude, the region between the horizontal line and the curve represents a certain allowable angle-of-attack that ensures the largest load indicator that results from trajectory design plus dispersions will not exceed the value already seen from winds. The horizontal line is below the peak of the curve to allow for some margin between the load indicators resulting from trajectory design and those resulting from wind dispersions.

Rogers and King [11] show how optimization using varying dynamic pressure and Q-α/Q-β limits leads to improved performance for the EHLLV. Gains of nearly 4000 lb$_m$ in payload to orbit were shown.

Fernandes et al. [12] describes a formulation, applicable to varying vehicles, for optimizing the open-loop portion of flight with a relatively small amount of software. However, the software requires such inputs as desired Q-α profile. This profile must be obtained through trajectory optimization. Also, Rogers and King [11] show that a change in constraints (as small a change as 30 psf in maximum dynamic pressure) leads to a significantly altered desirable Q-α profile (Fig. 3). Constraint curves such as those shown in Fig. 3 were designed for the different vehicles used in this study (based on data from MSFC's Structures and Dynamics Laboratory). NLS3 uses a constant constraint.

To allow for Q-α profile changes and to maintain a flexible solution, a slightly more complex procedure will be investigated here than in Fernandes et al. [12]. In this procedure, the pitchover is optimized with a number of constant pitch rates until the Q-α constraint curve is reached (similar to Fig. 3). Then this constraint curve is followed throughout the high dynamic pressure region. When the vehicle
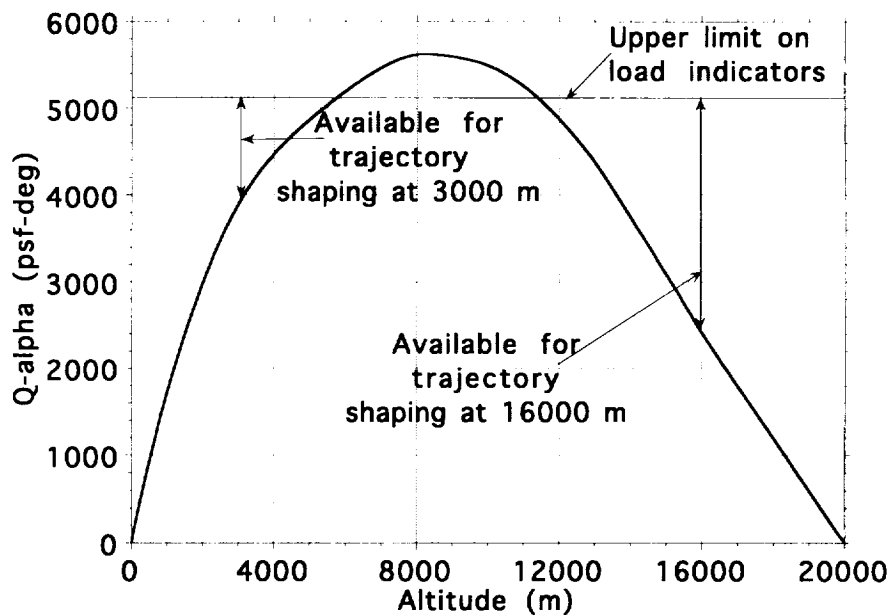

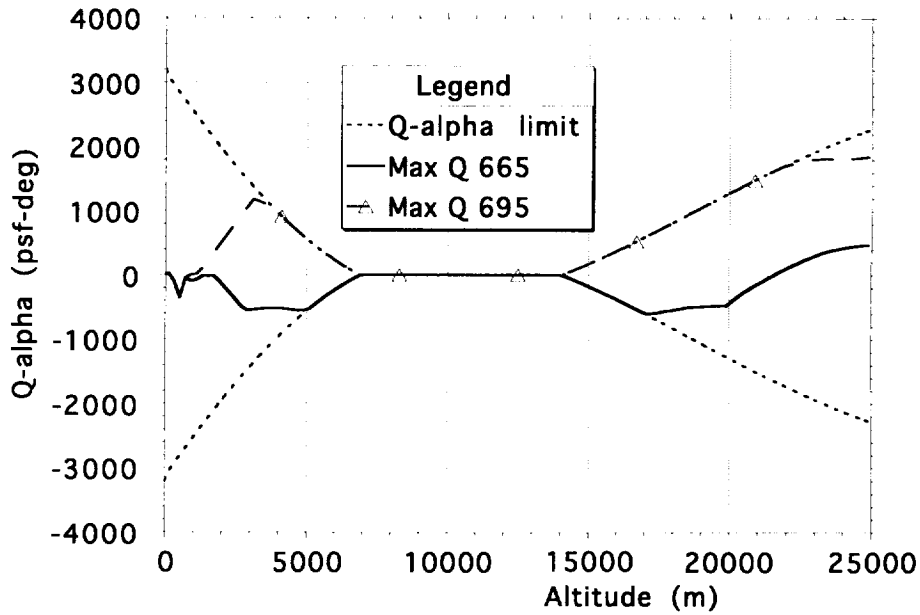FIG. 2. Typical Load Indicator Curve with Guidance Flexibility.

FIG. 3. Trajectory Design for Maximum Performance
with Load Indicator Limits (Early Heavy Lift Launch Vehicle).

can move off the minimum of the constraint curve, constrained vacuum closed-loop guidance takes over. Iterations on the initial pitchover parameters, the launch azimuth, and target node accomplish the optimization. Figure 4 shows a block diagram of this procedure. Results for this method will be given later.
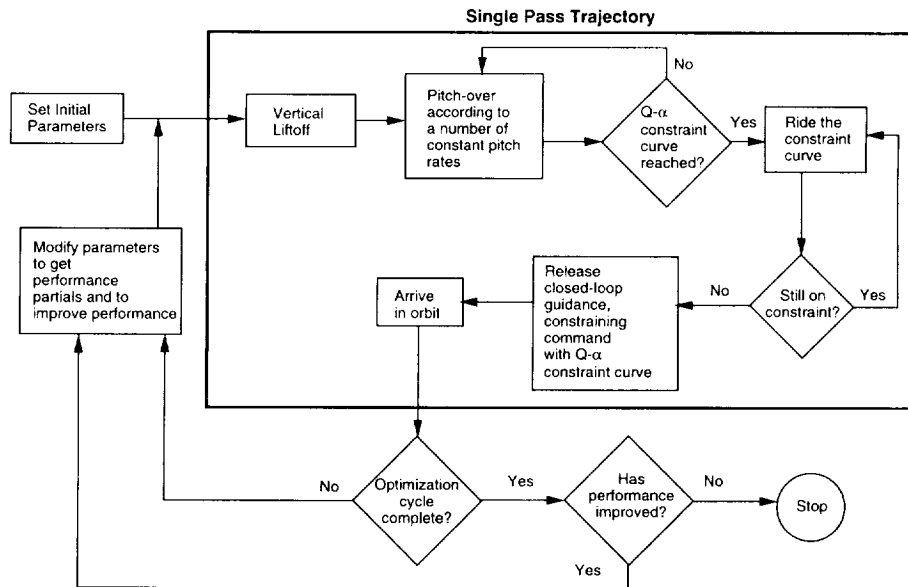

FIG. 4. Block Diagram of Methods 2 and 5. (Method 2 employs this scheme to design the optimal trajectory pre-launch. Method 5 employs this scheme to convergence once pre-launch, and then does a single optimization cycle once per second as a closed-loop guidance scheme.)

Method 3a: Early Release of Closed-Loop Guidance

MSFC studies show that vacuum closed-loop schemes can be released early (prior to vacuum flight), while avoiding increased load indicators by placing appropriate constraints on the commands. Early release yields an increased performance, if the open-loop portion is not optimal (that is, if optimized angles of attack are not used after maximum dynamic pressure). An example is an open-loop portion designed to fly at zero angle-of-attack from the high dynamic pressure region all the way to closed-loop release. If closed-loop release occurs in the vacuum, nonzero angles of attack could have been flown prior to this time. If the open-loop portion is optimal, then the performance improvement would not be seen in the nominal case. Early closed-loop release should adapt better to dispersions than optimal open-loop guidance with vacuum closed-loop release.

Using the load indicator constraint methods (described in the first paragraph of method 2) to allow early closed-loop guidance release (while maintaining reasonable loads after closed-loop release) yields the performance values in Table 4. Compared to IGM, early-release IGM (ERIGM) gives better performance, from very little to about two percent. If maximum load indicators are used as a measure, IGM and ERIGM are about equal. The table shows ERIGM higher, but with the dispersed Q-α values added in (see later in the paper for a discussion of the dispersions considered), the results are about the same (except for the effect of a higher maximum dynamic pressure). The ERIGM maximum dynamic pressure is between two and sixteen percent higher. More performance can be gained if IGM is released even earlier (Table 5). Maximum dynamic pressure can be constrained, with some loss in performance (but with a result still better than with IGM only). Note, from Table 5, that there is a smaller performance gain for vehicles that are more sluggish (see Table 1). Note that the optimized open-loop design, combined with early linear tangent release (method 2), yields generally the best performance.

Method 3a₁: Release of Closed-Loop Guidance during Solid Burns

The somewhat irregular thrust and flowrate patterns of solid rocket motors fluctuate too much to be modeled easily by closed-loop guidance schemes. Therefore, guidance release has generally been delayed until after solid rocket jettison on operational vehicles. Figure 5 shows the RSRM thrust and flow rate profile (furnished by MSFC's Propulsion Laboratory). Guidance schemes generally work best where the thrust and acceleration are constant or easily modeled.

To overcome this irregular thrust and flowrate pattern, the solid rocket burn was broken down into discrete segments. Over a small time period, average thrust and flowrate can be used for guidance. The guidance scheme can then model the solid rocket burn as a number of constant thrust stages. In reality, the guidance is assuming a thrust value that is lower than actual thrust for part of the time interval, and higher than actual thrust for the remainder of the time interval.

Breaking the solid burn down into small, average thrust/flowrate intervals allows guidance to be released earlier than the nominal 122 seconds (RSRM jettison) on EHLLV trajectories. Figure 6 shows the pitch profile for the nominal release time. Results indicate that releasing closed-loop guidance at 100 seconds provides a 743 lb_m payload improvement. The pitch profile for this case is also shown in

TABLE 4.   IGM at 140 s[1] versus Early Release IGM (100 s)

	NLS2AER	NLS2EO	EHLLV	NLS3US
	Performance (MECO mass-lb_m)			
IGM	219085	209278	324863	30251
ERIGM	219810	210479	325605	30261
Delta	+725	+1201	+742	+10
	Open-Loop Max Load Indicators (nominal) Q-α, Q-β (psf-deg)			
IGM	2717	793	1283	670
ERIGM	2878	832	1340	756
Delta	+161	+39	+57	+86
	Closed-Loop Max Load Indicators (nominal) Q-α, Q-β (psf-deg)			
IGM	80	683	135	1878
ERIGM	1803	5127	953	2203
Delta	+1723	+4444	+818	+325
	Excess Propellant Dispersion (lb_m, RSS-)			
IGM	−2854	−3115	−7515	−659
ERIGM	−3173	−3162	−7249	−663
Delta	−319	−47	+266	−4
	Open-Loop Load Indicator Dispersion Q-α, Q-β (psf-deg)			
IGM	3670	4204	3902	2712
ERIGM	3611	4336	3837	2682
Delta	−59	+132	−65	−30
	Closed-Loop Load Indicator Dispersion Q-α, Q-β (psf-deg)			
IGM	50	206	50	414
ERIGM	503	1058	1098	758
Delta	+453	+852	+1048	+344
	Maximum Dynamic Pressure (psf)			
IGM	724	773	651	482
ERIGM	750	884	665	534
Delta	+26	+111	+14	+52
	Launch Window Delta Minutes for 2000 lb_m penalty			
IGM	100		10	128[2]
ERIGM	100	120	10	120[2]
Delta	0	−3	0	−8[2]

[1] 121 s for EHLLV.
[2] 200 lb_m penalty.

Fig. 6. Further studies also show that releasing guidance after maximum dynamic pressure (at about 70 seconds) results in a 1784 lb_m improvement (Table 5). Note the smoother transition into closed-loop guidance in Fig. 6. The pitch curve is somewhat bumpy during the solid portion due to the approximation of the thrust trace. The small bump shortly after 300 seconds is due to the guidance being uninformed of the shroud drop.

TABLE 5. Comparison of Release Time Results[1]

	EHLLV	NLS2AER	NLS2EO	NLS3US
Time (s)	121	140	140	140
Performance (lb_m)	324 862	219 085	209 515	30 245
Time (s)	100	100	100	100
Performance (lb_m)	325 605	219 810	210 622	30 260
Time (s)	70	70	86	n/a
Performance (lb_m)	326 510	220 393	210 800	n/a
Time (s)	75	70	80	140
Optimal open-loop Performance (lb_m)	326 646	222 391	210 776	30 282

[1]Since maximum dynamic pressure for NLS3US is at about 100 seconds, earlier guidance release times were not used. Similarly, 70 seconds would be before maximum dynamic pressure for NLS2EO.

Releasing guidance this early into flight demands that aerodynamic loads be taken into account. For the EHLLV, the optimal pitch and yaw commands are modified based on the current allowable loads derived from the vehicle's approximate $Q\text{-}\alpha/Q\text{-}\beta$ dispersion profiles (see the first paragraph of method 2). So although the load indicators ($Q\text{-}\alpha$ and $Q\text{-}\beta$) were greater in the 70 second release case, they were well within design tolerances for this vehicle.

Method 3b: SATLIT

Spherical Atmospheric Linear Tangent (SATLIT) guidance [2,6] retains the atmospheric terms in the equations of motion and references the steering com-
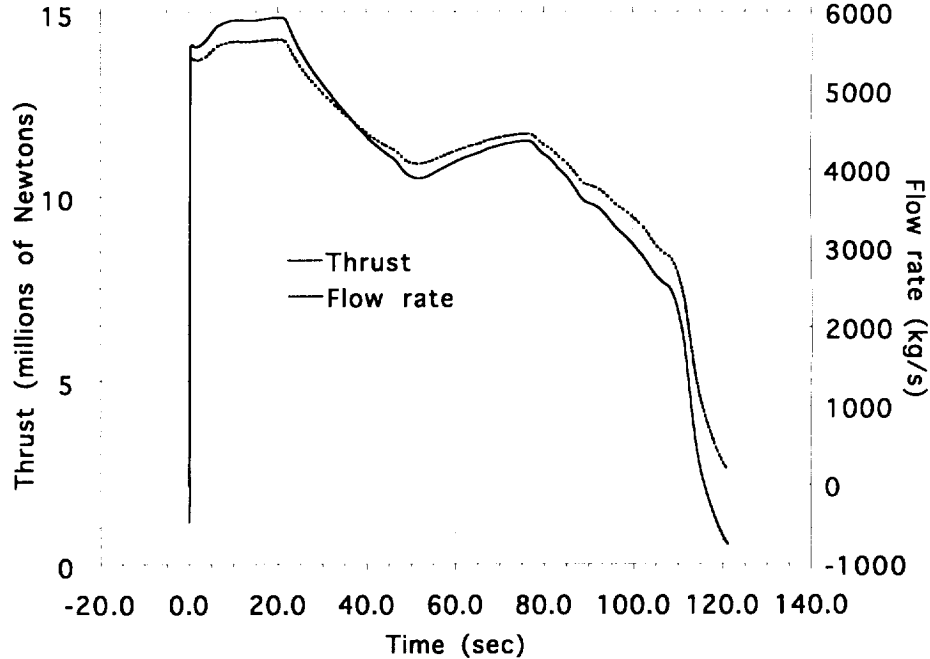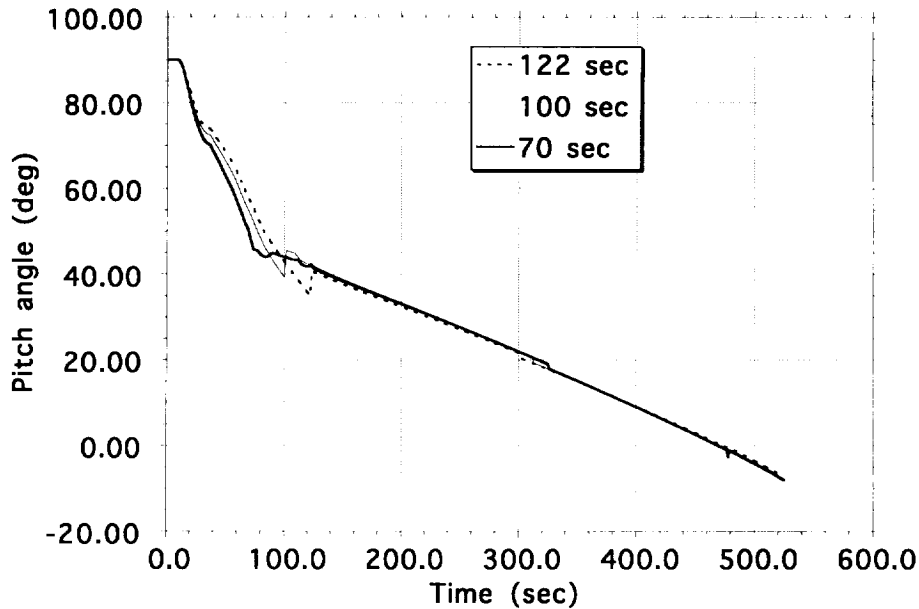

FIG. 5. RSRM Thrust and Flow Rate.

FIG. 6.   Pitch Profiles for EHLLV with Varying Guidance Release.

mands to the local horizontal. This hopefully allows for better performance (than for vacuum linear tangent steering) and for release of closed-loop guidance earlier in the flight. In practice, however, use of SATLIT did not yield any performance improvement. SATLIT was released at various times for the NLS2 vehicle with engine out at liftoff. Release times ranged from 30 seconds to 170 seconds after liftoff. No improvements were seen over use of the regular IGM, without the atmospheric terms. For example, SATLIT, with a release time of 50 seconds after liftoff, has a mass to orbit of $210\,544$ lb$_m$, with a max Q of 994 psf. The early-release IGM (ERIGM) result for NLS2EO with a guidance release of 70 seconds gave a mass to orbit of $210\,499$ lb$_m$, with a max Q of 908 psf (the simulation limited max Q to about 900 psf). Enabling the ERIGM case to have the same max Q as the SATLIT case (a limit of 994 psf) yielded a performance increase to $210\,739$ lb$_m$. The reason for this is two-fold: First, linear tangent steering is optimal for flight in a vacuum over a flat Earth. The presence of the atmosphere makes the assumption no longer valid, so that linear tangent steering very early is not optimal. In fact, the vehicle must pitch over at a more rapid rate before moving to the linear rate (see Fig. 1). Second, the presence of the atmospheric constraints during the high dynamic pressure region forces the trajectory to fly far off a linear tangent profile, so that the period before the constrained portion must set up the proper conditions for the constrained portion, rather than being forced to fly a linear tangent scheme.

Method 4: BOMAAG

Boundary Mapping Atmospheric Ascent Guidance (BOMAAG) [2,7,8] is designed by modeling the optimized vehicle ascent trajectory for a high thrust dispersion and for a low thrust dispersion. The resulting trajectories are then mapped into a functional form dependent on the vertical and horizontal velocity

profiles from the two design trajectories (Fig. 7). When the vehicle is in flight, the measured vertical and horizontal speeds are fed back into the guidance logic, which uses the functions to determine the desired pitch profile. This profile would presumably be closer to the optimal profile that would result if the dispersions that were actually seen were modeled in the trajectory design. A number of dispersions will behave like thrust dispersions in yielding an acceleration impact on the vehicle. The high and low thrust trajectories can be wind-biased, if desired.

Results in Table 6 show that BOMAAG is slightly worse for performance, when compared to ERIGM, the early-release of IGM (at 100 seconds). This is probably due to coarseness in BOMAAG modeling since the performance should be equal. The open-loop indicator differences are probably also due to coarseness. However, since BOMAAG is designed to high and low thrust profiles (as opposed to the nominal profile), it has some trouble hitting the nominal case exactly.

The closed-loop variations are due to a difference in handoff to the closed-loop guidance. Guidance did not need to have aerodynamic angles as high in some cases, and thus did not fly them as high. Note, however, that both are within the Q-α and Q-β constraints determined through method 2. The constraint curves for NLS2 allow for higher Q-α and Q-β values than those for the EHLLV and NLS3. BOMAAG reoptimized for zero angle-of-attack flight and will not necessarily yield better performance when there are dispersions, as can be seen in the table (see later for a listing of the dispersions considered).

Open-loop load indicator dispersions are a little better with BOMAAG, but the improvement is somewhat negated by the higher nominal indicators. Since
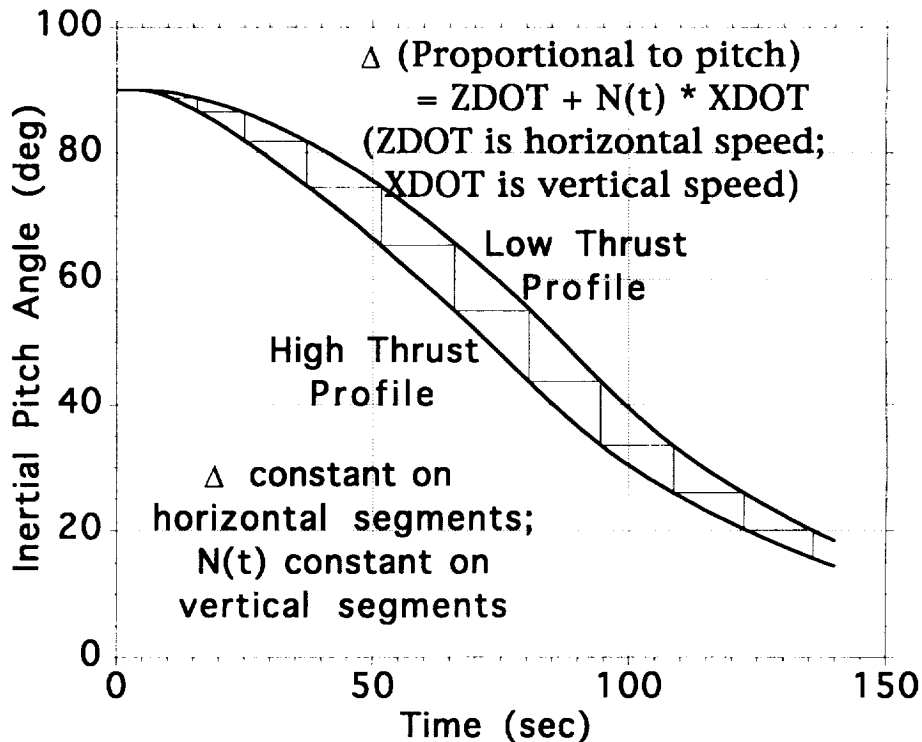

FIG. 7. BOMAAG Guidance.

TABLE 6. Early Release IGM (100 s) versus BOMAAG with IGM at 100 seconds
(EHLLV at 121 s)

	NLS2AER	NLS2EO	EHLLV	NLS3US
	Performance (MECO mass-lb_m)			
ERIGM	219810	210479	325605	30261
BOMAAG	219654	210348	325389	30259
Delta	−156	−131	−216	−2
	Open-Loop Max Load Indicators (nominal) Q-α, Q-β (psf-deg)			
ERIGM	2878	832	1340	756
BOMAAG	3235	961	1465	453
Delta	+357	+129	+125	−303
	Closed-Loop Max Load Indicators (nominal) Q-α, Q-β (psf-deg)			
ERIGM	1803	5127	953	2203
BOMAAG	1387	4478	947	1866
Delta	−416	−649	−6	−337
	Excess Propellant Dispersion (lb_m, RSS−)			
ERIGM	−3173	−3162	−7249	−663
BOMAAG	−3197	−3182	−9619	−674
Delta	−24	−20	−2370	−11
	Open-Loop Load Indicator Dispersion Q-α, Q-β (psf-deg)			
ERIGM	3611	4336	3837	2682
BOMAAG	3461	3972	3909	2619
Delta	−150	−364	+72	−63
	Closed-Loop Load Indicator Dispersion Q-α, Q-β (psf-deg)			
ERIGM	503	1058	1098	758
BOMAAG	516	2087	1377	912
Delta	+13	+1029	+279	+154
	Maximum Dynamic Pressure (psf)			
ERIGM	750	884	665	534
BOMAAG	735	854	651	500
Delta	−15	−30	−4	−34
	Low Thrust Delta Performance (lb_m)			
ERIGM	−571	−950	−5459[1]	−385
BOMAAG	−632	−1013	−8069[1]	−401
Delta	−61	−63	−2610[1]	−16
	Thrust Dispersion Largest Open-Loop Load Indicator Delta (psf-deg)			
ERIGM	117	54	320	187
BOMAAG	181	30	610	−15
Delta	+64	−24	+290	−202

[1]RSRM thrust dispersion.

closed-loop guidance uses indicator limits and the indicators were lower in the nominal case, there is more room for increase. The results are still within the indicator limits.

Maximum dynamic pressure is a little better for BOMAAG, but this results from the coarseness of the BOMAAG modeling. Low-thrust performance is worse for BOMAAG since the profile is reoptimized for zero angle-of-attack. BOMAAG should do better in the zero angle-of-attack region for load indicators with a thrust dispersion, but the open-loop indicators are not necessarily better since the region outside the zero angle-of-attack region might be worse for nominal winds. In any event, thrust dispersion loads are swamped by other (primarily wind) loads.

The bottom line is that BOMAAG does not help for the case where the design open-loop trajectory is zero angle-of-attack. Note also that BOMAAG is attempting to come back to the best possible pre-launch-designed profile if the dispersions were known pre-launch. But since the vehicle is already not on this trajectory, flying the pre-launch best pitch profile may no longer be optimal. BOMAAG could also be used with optimized open-loop trajectories. This was tested for the NLS2 with engine out, but the results were equivalent to those in Table 6.

Method 5: Optimized Closed-Loop Guidance in the Atmosphere

Using optimized open-loop profiles found with the open-loop optimization methods described earlier (method 2), one can design a relatively simple closed-loop scheme that emulates the same trajectory design philosophy, but has the advantage of taking into account dispersions that have occurred up to the current time. McDonnell Douglas has designed such a scheme for the Shuttle [12]. That guidance scheme iterates to hit desired staging targets that nearly optimize the trajectory. It makes use of desirable Q-α profiles.

For a new vehicle or for application to a variety of vehicles, the desired profile is not known beforehand. Changing the maximum dynamic pressure limit, for example, can significantly change the desired Q-α profile, as seen before. Thus the method used here for closed-loop atmospheric guidance is an adaptation of the method described in the open-loop optimization section of this paper (method 2), which is related to but more general than the scheme developed in Fernandes et al. [12]. This latter procedure would yield a smaller onboard software package for a single, mature launch vehicle.

In the closed-loop scheme developed under the current research, the trajectory is completely optimized prior to liftoff (using the procedure described earlier). Then, during the early ascent, and based on current navigation data, the trajectory takes one step each guidance cycle towards a better solution. This scheme will give the best performance possible of any closed-loop scheme released at liftoff, since it reoptimizes the entire trajectory at each guidance cycle. Figure 4 shows a block diagram of the procedure. Optimization ends after the vehicle enters the constrained region.

This procedure, used closed-loop onboard the vehicle, yields better results than open-loop guidance for the case of thrust dispersions. The gain is small however: 13 kg in a simulated NLS2EO case.

Unfortunately, the guidance commands large angles of attack during the high dynamic pressure region in the presence of a significant wind dispersion (angle of attack reached 6 degrees near max Q in a simulated case; this is much larger than the angle of attack that results from flying an open-loop profile to the dispersed wind). This results from the guidance designing to a different wind profile than the actual one.

One could use the navigated state vector to estimate the winds felt so far and then use this information in the optimization process. However, knowledge of the winds so far does not assist in knowing the winds ahead of the vehicle. Thus the closed-loop scheme cannot be trusted to adapt to inflight conditions if not told the current wind profile.

Suppose one couples the closed-loop scheme with a load-relief control system. This procedure will bring the loads back to a reasonable level in the presence of wind dispersions. However, this procedure also wipes out any performance advantage from the closed-loop guidance (In a simulated case, closed-loop performance with load relief was 44 kg less than open-loop performance with load relief.)

Suppose one uses day-of-launch wind data. In simulations performed using load relief, no load relief, varying numbers of pitchover parameters, and varying maximum dynamic pressure limits, closed-loop, optimal, constrained guidance did no better for performance or load indicators than did open-loop, optimal, constrained trajectory shaping.

Thus closed-loop atmospheric guidance does not improve loads or performance over open-loop guidance, whether or not the current wind conditions are known. Further, open-loop guidance gives cheaper onboard software. The big expense for onboard software is the software development and verification, not the size of the computer.

One argument for closed-loop guidance is the manpower expended to verify an open-loop design. However, it should be possible to automate the verification of an open-loop trajectory design, using computers on the ground that can run faster than those onboard. Thus increased manpower is not necessary for open-loop trajectory design. Closed-loop guidance onboard would reduce the number and complexity of parameters that require uploading to the vehicle on the ground (upload the wind profile only).

One possible advantage to a closed-loop scheme would be automatic adaptation to engine-outs and to aborts. However, the Shuttle uses open-loop procedures for these purposes, and it should be possible to automate these trajectory design procedures. The onboard scheme would, again, reduce the number of things requiring upload. The bottom line, though, is that no clear advantage for closed-loop guidance from liftoff has been observed.

Guidance Dispersion Results

Dispersion trajectories were generated for a number of the guidance schemes presented in this paper. For each guidance scheme/launch vehicle combination, the dispersions examined include engines, aerodynamics, winds, atmospheres, mass properties, and steering [13]. EHLLV dispersions also include the solid rocket boosters.

Liquid engine dispersions examined include thrust, specific impulse, mixture ratio, and thrust vector misalignment. Solid engine dispersions include thrust, specific impulse, propellant load, dry mass, thrust misalignment, and thrust imbalance between the two solid rocket motors. The solid rocket booster dispersion data files were provided by MSFC's Propulsion Laboratory. Aerodynamic dispersions include base forces and all coefficients. Most of these dispersions were $\pm 3\sigma$ in variation. Wind dispersions include 99% enveloping winds from each of the four

primary directions, as well as extreme winds taken from a set of 336 design extreme winds [14,15]. Hot and cold atmospheres were run, as were steering errors pitch and yaw. Mass properties dispersions include inert mass, propellant mass, and center of gravity dispersions.

Each of the dispersed values listed above constitute a single dispersion case. The optimized trajectory for that vehicle was flown with the dispersed value for the particular case, without guidance being aware of the dispersion. Each dispersion case would then give a dispersed value for MECO mass, max Q, max Q-α and Q-β (in both the open and closed-loop regions of flight), total heat, and maximum heat rate. These values were used as discriminators for the dispersion analyses. The dispersed values for each of the discriminators listed above were then gathered using root-sum-square sums (in plus and minus directions) to show an overall dispersion sensitivity of that particular guidance method. Charts were produced for absolute and relative results, effects at staging, and orbit targeting accuracy. Table 7 gives the root-sum-square results for dispersions for the different guidance schemes and vehicles that were examined.

The booster steering errors generally affected the accuracy of the orbit injection more than they affected the performance or the load indicators. However, the dispersions do not appear to be a clear discriminator between guidance schemes. The closed-loop load indicator dispersions are less when the closed-loop guidance (IGM) is released later, but this does not affect the overall maximum load indicators.

Summary and Conclusions

This paper contains results from ascent guidance studies conducted at the NASA Marshall Space Flight Center. The studies include investigation of different open-loop and closed-loop guidance schemes for a variety of potential launch vehicles. The focus is on operations cost, satisfaction of load indicator constraints, and maximization of performance. Results show that open-loop designs as a function of altitude or velocity are preferable to designs that are functions of time. Velocity results are slightly better than those for altitude.

Optimized open-loop trajectories can increase performance while maintaining load indicators within limits. Closed-loop atmospheric schemes that involve linear tangent steering or that involve feedback of velocity terms for trajectory modification did not yield any improvement. Early release of vacuum closed-loop guidance, including use during solid rocket booster operation, yielded some performance improvements. These improvements would decrease with use of optimized open-loop trajectories. Results show that optimized open-loop trajectories, coupled with early guidance release, yield good performance results.

Dispersion study results for several potential guidance schemes and launch vehicles are included in the paper. Results show that the nominal values of parameters of interest are affected more so than the dispersions. The primary cost driver is mission operations philosophy, not guidance scheme. No advantages were seen from use of closed-loop atmospheric ascent guidance as opposed to open-loop guidance, except that the number of parameters requiring verification on the ground and uploading to the vehicle would be reduced for closed-loop guidance. It should be possible to automate open-loop trajectory design and verification on the ground.

TABLE 7. Dispersion Results—RSS +/−

Vehicle Configuration/ Guidance Scheme	RSS +/−	Mass (lb$_m$)	Max Q (psf)	Open-loop Q-α (psf-deg)	Open-loop Q-β (psf-deg)	Closed-loop Q-α (psf-deg)	Closed-loop Q-β (psf-deg)	Total Heat (BTU/ft^2)	Max Heat Rate (heat/s)
EHLLV:									
IGM at 122 s	+	7034	109	2566	3903	50	40	20	0.25
	−	7515	74	540	72	69	14	18	0.20
IGM at 100 s	+	6620	115	2417	3837	1098	177	25	0.30
	−	7249	75	544	87	697	41	27	0.30
IGM at 70 s	+	5511	125	2198	3928	977	794	64	0.78
	−	7536	85	643	90	1248	486	22	0.31
BOMAAG	+	7022	148	3077	3817	327	40	71	0.87
IGM at 121 s	−	9796	98	656	83	122	7	51	0.61
Optimal Open	+	5520	126	2810	3372	908	590	53	0.65
IGM at 75 s	−	7482	85	417	449	1209	70	23	0.32
NLS2AER:									
IGM at 140 s	+	2625	118	2139	3670	50	46	52	0.73
	−	2854	69	576	165	45	4	56	0.95
IGM at 100 s	+	2579	128	2100	3611	446	503	59	0.83
	−	2911	84	571	185	434	54	64	1.08
IGM at 70 s	+	2630	144	2028	3641	961	1309	67	0.99
	−	2962	99	829	240	1095	26	55	0.91
BOMAAG	+	2627	132	2117	3599	946	255	56	0.82
IGM at 100 s	−	2942	84	574	264	844	470	58	0.98
Optimal Open	+	2710	127	2727	4086	1010	1399	58	0.82
IGM at 70 s	−	2877	65	631	162	836	11	62	1.03
NLS2EO:									
IGM at 140 s	+	2928	125	4203	3292	141	206	100	1.66
	−	3114	89	24	258	27	241	109	1.83
IGM at 100 s	+	3037	141	4336	2916	1058	751	133	1.94
	−	3174	94	27	324	24	993	138	2.12
IGM at 86 s	+	3048	142	4272	2860	725	1417	126	1.83
	−	3173	95	29	330	1231	993	122	1.90
BOMAAG	+	3074	147	4305	3207	462	1203	122	1.72
IGM at 100 s	−	3182	93	27	101	635	1654	124	1.96
Optimal Open	+	3064	142	4369	3437	1356	1760	131	1.81
IGM at 80 s	−	3154	95	28	73	18	862	112	1.77
NLS3US:									
IGM at 140 s	+	640	78	2713	2494	414	290	109	1.62
	−	659	48	303	34	420	308	108	1.62
IGM at 100 s	+	672	79	2682	2487	758	803	113	1.56
	−	663	53	470	73	626	556	111	1.56
BOMAAG	+	660	78	2619	2685	912	761	97	1.42
IGM at 100 s	−	674	48	296	12	812	557	100	1.48
Optimal Open	+	652	82	2745	2624	412	276	86	1.32
IGM at 140 s	−	662	51	401	5	371	22	89	1.38

Acknowledgment

References

[1] BORDANO, A.J., McSWAIN, G.G., and FERNANDES, S.T. "Autonomous Guidance, Navigation and Control," Paper No. 91-022, 14th AAS Guidance and Control Conference, Keystone, Colorado, February 1991.

[2] HANSON, J.M., SHRADER, M.W., CHANG, H.P., and FREEMAN, S.E. "Guidance and Dispersion Studies of National Launch System Ascent Trajectories," Paper No. 92-4306, AIAA Guidance and Control Conference, Hilton Head Island, South Carolina, August 1992.

[3] SMITH, I.E. "General Formulation of the Iterative Guidance Mode," NASA TMX-53414, March 22, 1966.

[4] McHENRY, R.L., BRAND, T.J., LONG, A.D., COCKRELL, B.F., and THIBODEAU, J.R. "Space Shuttle Ascent Guidance, Navigation, and Control," *Journal of the Astronautical Sciences,* Vol. 27, No. 1, January–March 1979, pp. 1–38.

[5] BROWN, K.R., HARROLD, E.F., and JOHNSON, G.W. "Rapid Optimization of Multiple-Burn Rocket Flights," NASA CR-1430, September 1969.

[6] CHANG, H.P. "Spherical Atmospheric Linear Tangent (SATLIT) Guidance," NASA MSFC Contract NAS 8-37814 Report, Sverdrup Technology, Inc., Huntsville, Alabama, March 1993.

[7] DEATON, A.W., and KELLEY, P.B. "Structural Load Reduction of the Space Shuttle Booster/Orbiter Configuration Using a Load Relief Guidance Technique," NASA TMX-64738, April 1973.

[8] PAVELITZ, S. "Evaluation of Boundary Mapping Atmospheric Ascent Guidance (BO-MAAG)," NASA MSFC Contract NAS 8-37814 Report, Sverdrup Technology, Inc., Huntsville, Alabama, May 1993.

[9] SKALECKI, L., and MARTIN, M. "General Adaptive Guidance Using Nonlinear Programming Constraint Solving Methods (FAST)," Paper No. 91-2820, AIAA Guidance, Navigation, and Control Conference, New Orleans, Louisiana, August 1991.

[10] LEUNG, M.S.K., and CALISE, A.J. "A Hybrid Approach to Near-Optimal Launch Vehicle Guidance," Paper No. 92-4304, AIAA Guidance and Control Conference, Hilton Head Island, South Carolina, August 1992.

[11] ROGERS, J.H., and KING, T.A. "Ascent Trajectory Optimization," IR&D Project 13302, FY93 Final Report, Rockwell International Space Systems Division, Huntsville Operations, September 1993.

[12] FERNANDES, S.T., FINK, C., and PESEK, D. "A Benchmark Guidance, Navigation and Control System for Future Launch Vehicles," McDonnell Douglas Space Systems Company Transmittal Memo TM-5.23.7.10-233, NASA JSC Contract NAS9-17885, September 1992.

[13] FREEMAN, S. "Ascent Guidance Trade Study Dispersion Results," NASA MSFC Contract NAS 8-37814 Report 222-025-93-009, Sverdrup Technology, Inc., Huntsville, Alabama, June 1993.

[14] CHANG, H.P. "Effect of NTI 336 Wind Profiles on EHLLV Ascent Performance," NASA MSFC Contract NAS 8-37814 Report, Sverdrup Technology, Inc., Huntsville, Alabama, December 1992.

[15] SMITH, O.E., ADELFANG, S.I., and BATTS, G.W. "Wind Models for the NLS Ascent Design," New Technology, Inc., Huntsville, Alabama, January 1992.